Lattice axial ratio and large uniaxial magnetocrystalline anisotropy in $L1_0$-type FePd single crystals prepared under compressive stress

H. Shima,[1,*] K. Oikawa,[2] A. Fujita,[1] K. Fukamichi,[1] K. Ishida,[1] and A. Sakuma[3]
[1]*Department of Materials Science, Graduate School of Engineering, Tohoku University, Aoba-yama 02, Sendai 980-8579, Japan*
[2]*National Institute of Advanced Industrial Science and Technology, Sendai 983–8511, Japan*
[3]*Department of Applied Physics, Graduate School of Engineering, Tohoku University, Aoba-yama 08, Sendai 980-8579, Japan*
(Received 28 March 2004; revised manuscript received 14 July 2004; published 8 December 2004)

$L1_0$-type FePd single crystals with a high order degree were prepared by ordering under compressive stress. Experimental and theoretical investigations on the relation among the axial ratio, *d* electron number and magnetocrystalline anisotropy energy (MAE) in $L1_0$-type FePd single crystals have been carried out. In the concentration dependence of the lattice constants, the *a* axis exhibits a strong dependence, compared with that of the *c* axis. As a result, the ratio of c/a decreases with increasing Pd concentration. The uniaxial magnetocrystalline anisotropy constant K_U at the equiatomic composition is evaluated to be 2.1×10^7 erg/cm^3 at 4.2 K and 1.7×10^7 erg/cm^3 at 300 K. The MAE becomes weaker as the ratio of c/a is apart from unity at higher Pd compositions. The calculated results by the first principles calculations with the LMTO-ASA including the spin-orbit coupling for the MAE of $L1_0$-type $Fe_{50}Pd_{50}$ are in accord with the present experimental results. The increase in the *d* electron number due to the increase of the Pd concentration facilitates the decrease of the MAE, cooperating with the decrease in the axial ratio c/a.

DOI: 10.1103/PhysRevB.70.224408 PACS number(s): 75.30.Gw, 71.20.Be, 75.50.Bb

I. INTRODUCTION

FePd alloys in the vicinity of the equiatomic composition transform from the disordered fcc phase to the ordered $L1_0$ phase with the axial ratio c/a less than unity.[1] $L1_0$-type FePd alloys have a large magnetocrystalline anisotropy energy due to the tetragonal symmetry, and hence they have extensively been studied as one of the promising materials for ultrahigh dense magnetic storage media.[2–7] Magnetic properties of $L1_0$-type FePd thin films,[2–4] nanoparticles,[5,6] and nanofabricated structures[7] have been investigated, and their large magnetic anisotropy and high coercivity in those systems bring about their potentiality for magnetic storages. The effective stable reading and writing volume *V* for magnetic storage media at temperature *T* can be evaluated by considering the ratio of the thermal fluctuation to the magnetocrystalline anisotropy energy K_UV/k_BT, where k_B is the Boltzmann constant and K_U is the uniaxial magnetic anisotropy constant. The volume *V* can be decreased by increasing the value of K_U, and hence the storage density of information becomes high. Thus, the precise evaluation of K_U is essential in order to develop excellent magnetic storage media. However, the lattice mismatch between FePd thin film and a substrate, the shape of FePd nanoparticles and nanofabricated structures significantly alter their magnetic properties from those of $L1_0$-type FePd bulk alloys due to the magnetoelastic coupling, surface and shape anisotropies.

In previous studies on $L1_0$-type FePd bulk alloys, the uniaxial magnetocrystalline anisotropy constant K_U for FePd alloys has been estimated to be the order of 10^7 erg/cm^3.[8–10] In detail, Kussmann and Müller studied the annealed polycrystalline $Fe_{50}Pd_{50}$ alloy and estimated the room temperature value of K_U to be 2.6×10^7 erg/cm^3 by analyzing the magnetization curves.[8] Miyata *et al.* carried out the magnetization measurements for quasisingle crystal FePd alloys at 4.2 K under magnetic fields up to 100 kOe and showed the Fe concentration dependence of K_U in $L1_0$-type FePd system.[9] However, $L1_0$-type FePd alloys exhibit multivariant microstructures to cancel the tetragonal distortion energy during ordering.[11–13] Therefore, the *c* axis in the $L1_0$-phase aligns parallel to the $\langle001\rangle$ directions in the fcc phase and three kinds of variants with different orientations of the *c* axis are conjugated. The magnetic properties such as magnetocrystalline anisotropy are strongly affected by the microstructure of the system because the *c* axis is the easy axis of magnetization. The magnetization measurements for single variant $L1_0$-type FePd alloys were made by Yermakov and Maykov, and the temperature and composition dependences of K_U were discussed.[10] By assuming the fourth order anisotropy constant $K_2=0$, the value of the second order anisotropy constant K_1 was indirectly calculated by a Sucksmith-Thompson (ST) method for the magnetization curves under the magnetic fields up to 20 kOe, although the strength of magnetic field was not enough for saturation.

In the present paper, the value of K_U is directly evaluated from the difference between the magnetization energy along the *a* and *c* axes in the single variant $L1_0$-type FePd alloys. Since the large magnetocrystalline anisotropy in $L1_0$-type FePd alloys is originated from the tetragonal crystal structure and the spin-orbit coupling, the axial ratio c/a, and the electronic state in the system dominate the magnetocrystalline anisotropy. When the Pd concentration is changed, it is expected that the axial ratio c/a is changed because the atomic radius of the Pd atom is larger than that of Fe. In addition, the *d* electron number can also be changed by the Pd concentration. Investigation on the concentration dependence of magnetic properties of $L1_0$-type FePd system can clarify the crystallographic and electronic origins of the magnetocrys-

 ©2004 The American Physical Society

talline anisotropy. In the present paper, the effects of Pd concentration on the axial ratio c/a and the magnetocrystalline anisotropy constant are discussed on the basis of the experimental results and first principles calculations. For reliable calculations, all the present calculations have been performed for the equiatomic $L1_0$-type $Fe_{50}Pd_{50}$ in the fully atomic ordered state. The axial ratio c/a and band filling q are varied in the calculations in order to investigate the effects on the MAE.

II. EXPERIMENTS AND CALCULATION METHOD

$Fe_{100-x}Pd_x$ single crystals with the Pd content $x=50$, 53, 55, and 57 at. % were grown by a floating zone method in a purified He atmosphere. After homogenization at 1473 K for 24 hours in evacuated quartz tubes, the single crystals were oriented by the backscattering Laue method and electron backscatting pattern (EBSP) method. The crystals were cut into a cubic shape with all the faces parallel to the {001} planes in the fcc phase. The order-disorder transformation temperature was evaluated with the differential scanning calorimeter. The heat treatment for ordering was made under a compressive stress of 20–25 MPa using a high temperature compression testing machine, followed by a furnace cooling.[14,15] The lattice constants in the $L1_0$ phase were determined by x-ray diffractions for the single variant $L1_0$-type FePd alloys. The alloy compositions were determined by wavelength dispersion x-ray spectroscopy. The magnetization measurements at 4.2 K were carried out with a superconducting quantum interference device (SQUID) magnetometer in the magnetic field up to 55 kOe.

The first principles calculations including the spin-orbit interaction for $L1_0$-type FePd were performed by the linear-muffin-tin orbital (LMTO) method with the atomic sphere approximation (ASA) based on the local spin density approximation (LSDA).[16] According to the force theorem within LSDA,[17,18] the MAE between the two different magnetization directions is given by the following total energy difference in the occupied eigenstate of the Kohn-Sham equation,

$$\mathrm{MAE} = \sum_{i,k}^{\mathrm{occ}} \varepsilon_i(\mathbf{m}[\mathbf{n}_1],\mathbf{k}) - \sum_{ik}^{\mathrm{occ}} \varepsilon_i(\mathbf{m}[\mathbf{n}_2],\mathbf{k}), \qquad (1)$$

where $\varepsilon_i(\mathbf{m}[\mathbf{n}],\mathbf{k})$ denotes the eigenvalues with the band index i when the local spin density of magnetization $\mathbf{m}[\mathbf{n}]$ directs the crystallographic orientation $\mathbf{n}$.

III. RESULTS AND DISCUSSION

The backscattering Laue patterns gave clear spots, showing that all the fcc specimens are in a single crystal state. By analyzing the EBSP patterns, the single crystals were cut into a cubic shape with six {001} planes. The orientation error in the cubic shape specimens is within ±1°. In the x-ray diffraction patterns after ordering, only the peaks from the {001} planes were observed when the scattering vector is parallel to the compressive stress during ordering, showing the clear evidence for a single variant $L1_0$ phase. Figures 1(a) and 1(b)

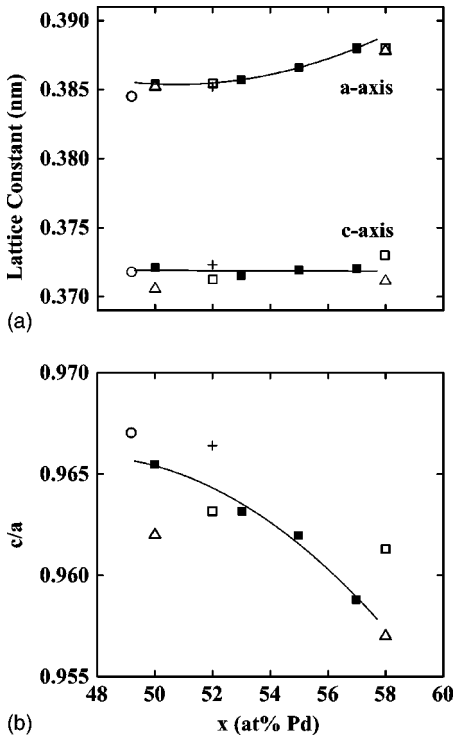

FIG. 1. The Pd concentration dependence of (a) the lattice constants a and c and (b) the axial ratio c/a. The solid squares (■) stand for the present data. The previously reported data are given by the symbols of □ (Ref. 9), ○ (Ref. 12), △ (Ref. 19), and + (Ref. 21).

show the Pd concentration dependence of the lattice constants a and c, and the axial ratio c/a in the $L1_0$-type $Fe_{100-x}Pd_x$ system. For comparison, the available previous data of a, c, and c/a (Refs. 9, 12, 19, and 21) are also shown in the same figures. The a axis elongates, whereas the c axis hardly changes with increasing Pd concentration x. The value of c/a decreases with increasing Pd concentration. Comparing with the lattice constant a_0 for the fcc-type FePd, the relation $a > a_0 > c$ is observed. The unit cell volume decreases after ordering. From the phase transformation experiment, the order persists up to about 1053 K at $x=60$.[20] The $L1_0$-phase stability at higher value of x corresponds to the decrease of c/a with increasing x. The values of a and c, and the axial ratio c/a measured for $L1_0$-type $Fe_{100-x}Pd_x$ single crystals agree with those values measured for powdered and long-time annealed specimens.[19,21] The degree of order η is defined as

$$\eta^2 = \frac{(I_{001}/I_{002})_{\mathrm{experiment}}}{(I_{001}/I_{002})_{\mathrm{calculation}}}, \qquad (2)$$

where I_{001} and I_{002} are the integrated intensities of 001 superlattice and 002 fundamental diffractions. For calculations of the values of $(I_{001}/I_{002})_{\mathrm{calculation}}$, the structure factors were defined as

$$F_{(001)} = 2\{f_{\mathrm{Fe}}(\theta_{001}) - f_{\mathrm{Pd}}(\theta_{001})\} \qquad (3)$$

for 001 diffraction and

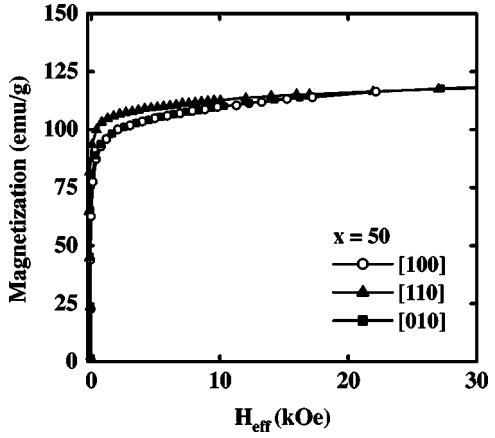

FIG. 2. The magnetization curves at 4.2 K for fcc-type $Fe_{50}Pd_{50}$. The symbols ○, ▲, and ■ correspond to the results of the [100], [110], and [010] directions, respectively.

$$F_{(002)} = 2\{f_{Fe}(\theta_{002}) + f_{Pd}(\theta_{002})\} \tag{4}$$

for 002 diffraction. Here, $f_i(\theta_{klm})$ is the atomic scattering factor of the element i from (hkl) plane at the angle $2\theta_{hkl}$. The integrated intensity I_{hkl} is proportional to $|F_{hkl}|^2$. Here, the Lorentz polarization factor is taken into account, whereas the corrections by the absorption and the temperature factors are neglected. The experimental degree of order for the $L1_0$-type $Fe_{50}Pd_{50}$ was evaluated to be about 0.9. The value of $c/a=0.966$ at the equiatomic composition $x=50$ is the evidence for the high degree of the long-range atomic order. The rate of the ordering becomes over 10 times faster by applying the compressive stress.[22] In addition, the long-range order parameter η in the $L1_0$-type binary alloys keeps fairly high value up to the order-disorder transformation temperature.[23] Consequently, the high degree of the long-range order at each composition can be achieved up to the end of a furnace cool under a compressive stress. Considering the temperature dependence of the long-range order, there is no significant difference between the axial ratio at 300 K and that at 4.2 K. At a constant temperature, K_U is a function of the Pd concentration x, the axial ratio c/a, and the long-range order parameter η as $K_U=K_U(x,c/a,\eta)$. Generally, the value of η is parametrized by the axial ratio c/a and the alloy composition.[24,25] Therefore, two adopted variables, the axial ratio c/a and the Pd concentration x, suffice for discussion of the MAE.

The magnetization curves for the fcc-type $Fe_{50}Pd_{50}$ at 4.2 K are shown in Fig. 2. The magnetic fields were applied along the [100], [110], and [010] directions. No remarkable differences between the magnetization curves along the [100] and [010] directions are observed, because the [100] and [010] directions are crystallographically equivalent. The magnetization curve along the [110] direction is saturated under slightly lower field compared with the curves along the [100] and [010] directions. From the magnetization curves for the fcc-type $Fe_{50}Pd_{50}$ single crystal in Fig. 2, the magnetocrystalline anisotropy constant in the fcc-type $Fe_{50}Pd_{50}$ is estimated to be the order of 10^5 erg/cm^3. On the contrary, a large uniaxial magnetocrystalline anisotropy is observed in $L1_0$-type $Fe_{100-x}Pd_x$ as shown in Figs. 3(a)–3(d). The coercivity is relatively low, which is also observed in the multivariant $L1_0$-type $Fe_{50}Pd_{50}$.[11] In the $L1_0$-type FePd system, the density of antiphase boundary (APB) is higher than other ordered binary alloys. However, the displacement of the magnetic domain wall takes place through the APB without pinning. The initial magnetization curves along the a and c axes are different from those for the multivariant, or quasisingle crystal $L1_0$-type $Fe_{50}Pd_{50}$.[12,13] Carrying out the heat treatment for ordering under compressive stress, the c axis of

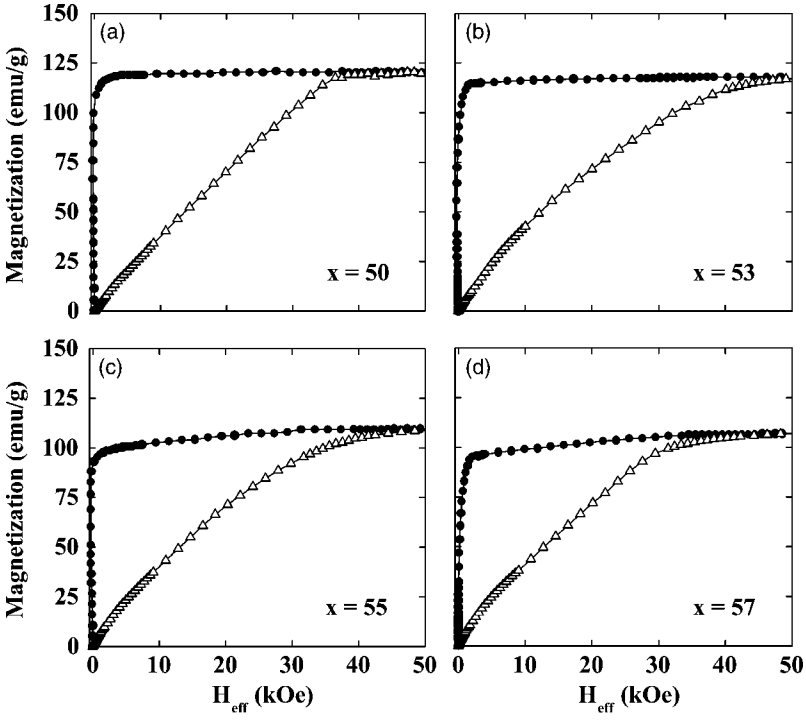

FIG. 3. The magnetization curves at 4.2 K for $L1_0$-type $Fe_{100-x}Pd_x$ alloys. The open triangle (△) and the solid circle (●) stand for the values measured along the a- and c-axis directions, respectively.

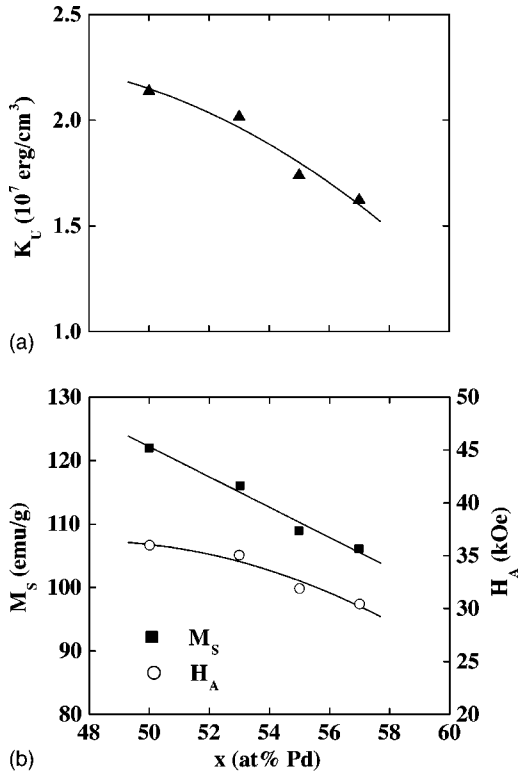

FIG. 4. The Pd concentration dependence of (a) the uniaxial magnetocrystalline constant K_U, (b) the anisotropy field H_A, and the saturation magnetization M_S.

the magnetization easy axis selectively aligns parallel to the direction of the compressive stress.[15] Therefore, the high magnetic field is necessary to saturate along the *a* axis, whereas the magnetization along the *c* axis is immediately saturated under a low magnetic field of several hundred Oe.

The uniaxial magnetocrystalline anisotropy constant K_U for $L1_0$-type $Fe_{100-x}Pd_x$ is evaluated as the difference between the Helmholtz magnetic free energy along the *a* and *c* axes. The value of K_U is defined by

$$K_U = \int_0^{M_S} (H_{a\text{-axis}} - H_{c\text{-axis}})dM, \tag{5}$$

where M_S is the saturation magnetization and $H_{a\text{-axis}}$ and $H_{c\text{-axis}}$ indicate the applied external magnetic fields along the *a*- and *c*-axes directions, respectively. The Pd concentration dependence of the value of K_U is given in Fig. 4(a). Figure 4(b) shows the saturation magnetization M_S at 4.2 K and the anisotropy field H_A given by $H_A = 2K_U/M_S$ as a function of Pd concentration. The value of K_U at $x=50$ is evaluated to be 2.1×10^7 erg/cm^3 (2.1×10^6 J/m^3) at 4.2 K. The uniaxial magnetocrystalline anisotropy becomes weaker at higher Pd concentrations. The value of M_S monotonically decreases with increasing *x*. The value of K_U in the present experiment is given in Table I, together with the previous data for comparison. The value of $K_U = 2.6\times10^7$ erg/cm^3 at room temperature reported by Kusshmann and Müller may be overestimated, though the errors of ±15% were taken into account. In the case of the Sucksmith-Thompson (ST) method obtained by Yermakov and Maykov[10] for the magnetization curves along the *a* axis, the value of K_U is about 6% larger than the present results, which is the limit of error for the fitting as pointed out by the authors. According to the magnetic domain observation by a Bitter method for $L1_0$-type FePd single crystal, most of the magnetizations in remanence are parallel to the *c* axis due to the strong magnetocrystalline anisotropy.[26] Therefore, a high magnetic field is necessary for the complete domain wall annihilation when the magnetic field is applied to the *a*-axis direction. On the other hand, the ST method is premised on the coherent magnetization rotation, and hence the error in K_U is retained when the ST method is applied to the magnetization curves along the *a* axis in low magnetic fields,[10,24] even if the specimens are in the single crystal state. Figure 5 shows the vector magnetization curves at 4.2 K for $L1_0$-type $Fe_{50}Pd_{50}$. The notations M_L and M_T, respectively, represent the longitudinal and transverse components of magnetization against the external magnetic field direction, and then M is given by $M=\sqrt{M_L^2+M_T^2}$. The values of M_L, M_T, and M in Fig. 5 are

TABLE I. The experimental values of K_U, M_S, and H_A for $L1_0$-type FePd alloys, together with the previous data (Refs. 8–10, 24, and 27).

at. % Pd	K_U (10^7 erg/cm^3)	M_S (emu/cm^3)	H_A (kOe)	Remark	Reference
50	2.6 (at RT)	1090		Polycrystal	8
50	2.2 (at 4.2 K)	1170		Single crystal, ST method up to 20 kOe	10
50	2.1 (at 4.2 K)	1190	36	Single crystal, Integration up to 55 kOe	Present results
50	1.9 (at 300 K)	1134	35.2	Single crystal, ST method up to 30 kOe	24
50	1.8 (at 300 K)	1100	33	Polytwind crystal Kronmüller analysis	28
52	2.08 (at 4.2 K)	1048	39.7	Quasisingle crystal	9

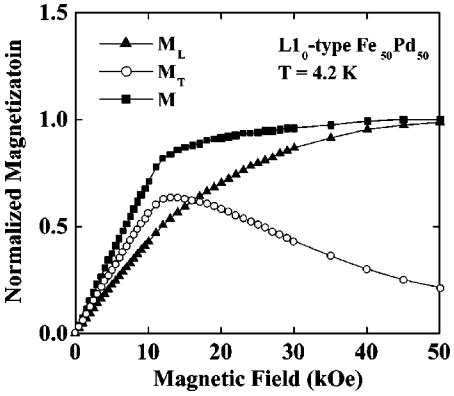

FIG. 5. The vector magnetization curves at 4.2 K for $L1_0$-type $Fe_{50}Pd_{50}$ alloy. The notations M_L (▲) and M_T (○) are the longitudinal and transverse components of magnetization against the external magnetic field, respectively. The symbol ■ designates the absolute value of vector magnetization.

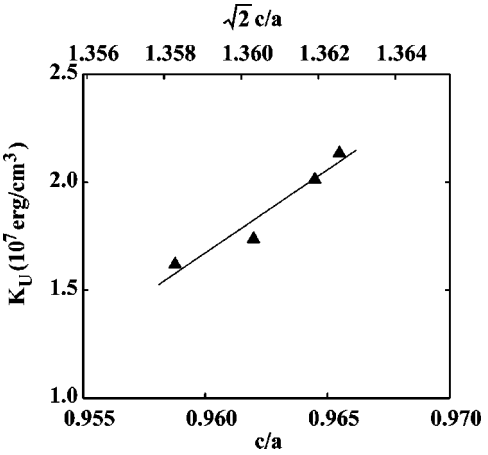

FIG. 6. The uniaxial magnetocrystalline anisotropy constant K_U as a function of the axial ratio c/a for $L1_0$-type $Fe_{50}Pd_{50}$ alloy.

normalized to M_S. In the magnetic field less than 30 kOe, the value of M gradually increases with the strength of applied magnetic field, showing the existence of residual magnetic domain walls. It should be noted that the residual magnetic domain walls cause the difference in the evaluated value of K_U, depending on the methods of analysis used. For example, Kronmüller's analysis was applied to the magnetizaiton curves of $L1_0$-type $Fe_{50}Pd_{50}$ at 300 K,[27] and the evaluated values of K_U, M_S, and H_A are all different from those evaluated by the ST method.[24]

In our recent paper, the temperature dependence of MAE has been discussed.[28] The value of K_U for the $L1_0$-type $Fe_{50}Pd_{50}$ single crystal decreases with increasing temperature, showing a relation of $K_U(T) \propto M_S(T)^{3.3}$. The power law for the temperature dependence of K_U agrees with the case of the uniaxial crystal symmetry in the Callen-Callen model.[29] The value of K_U at 300 K evaluated from Eq. (5) is 1.7×10^7 erg/cm^3, retaining a large value of K_U up to room temperature.

The uniaxial magnetocrystalline anisotropy constant K_U as a function of c/a is plotted in Fig. 6. The bottom abscissa is the axial ratio c/a in the $L1_0$ structure and the top abscissa is the axial ratio $\sqrt{2}c/a$ in the tetragonally distorted B2 representation, whose relation is illustrated in Fig. 7. The value of K_U decreases when the axial ratio c/a goes away from unity. What must be noticed is that the axial ratio $\sqrt{2}c/a$ approaches unity with decreasing the value of K_U in consideration of the B2 representation. The symmetry of the atomic ordering in the $L1_0$ structure is still uniaxial at $c/a=1$ because of the layered structure of Fe and Pd atoms along the c-axis direction. Note that the decrease of K_U at higher Pd concentrations corresponds to the reduction of the ratio of tetragonality in the B2 representation, that is, the B2 structure with the axial ratio $\sqrt{2}c/a=1$ has a cubic symmetry. Consequently, the magnetocrystalline anisotropy becomes weak.

The density of states (DOS) curves calculated by the LMTO-ASA method for the Fe and Pd in $L1_0$-type $Fe_{50}Pd_{50}$ are given in Fig. 8. The majority spin Fe and Pd bands as well as the minority spin Pd d bands are fulfilled. The value of the magnetic moment is evaluated to be 3.04 μ_B/atom for Fe, larger than that of the bulk bcc Fe, indicating the enhancement of the magnetic moment by a strong hybridization between Fe and Pd d bands. Since the minority spin d orbitals of Fe and Pd overlap in a wider range of real space compared with the majority spin d bands, the minority spin d electrons strongly hybridize. In addition, the gravity center of the minority spin d bands of Fe is slightly higher than that of Pd. As a result, the minority spin d bands of Fe are markedly shifted above E_F by the exchange splitting and the magnetic moment of Fe is enhanced.

In the $L1_0$-type $Fe_{100-x}Pd_x$ alloys, the spin-orbit coupling is strongly correlated with the magnetocrystalline anisotropy. The present spin-orbit interaction parameter for Pd is about 3 times larger than that of Fe in both the majority and minority orbitals in the present calculation, bringing about the large magnetocrystalline anisotropy. Shown in Fig. 9 is the MAE of the $L1_0$-type $Fe_{50}Pd_{50}$ as a function of the axial ratio c/a. The solid triangle (▲) is the experimental result for $x=50$. The total energy surface consisting of the eigenvalues in Eq. (1) depends on both the axial ratio c/a and the unit cell volume ca^2 (Ref. 30). In the present calculations, the value

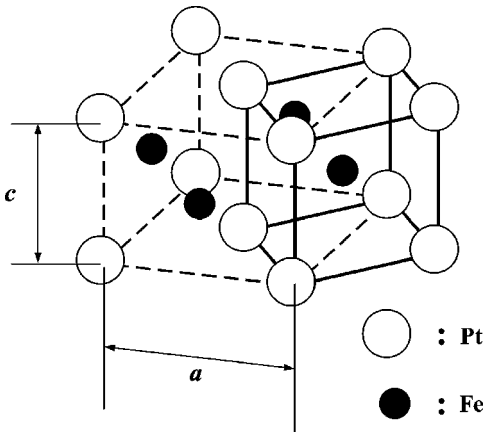

FIG. 7. The structural relation between the $L1_0$ and B2 representations. The dashed and solid lines represent the $L1_0$ and B2 structures, respectively.

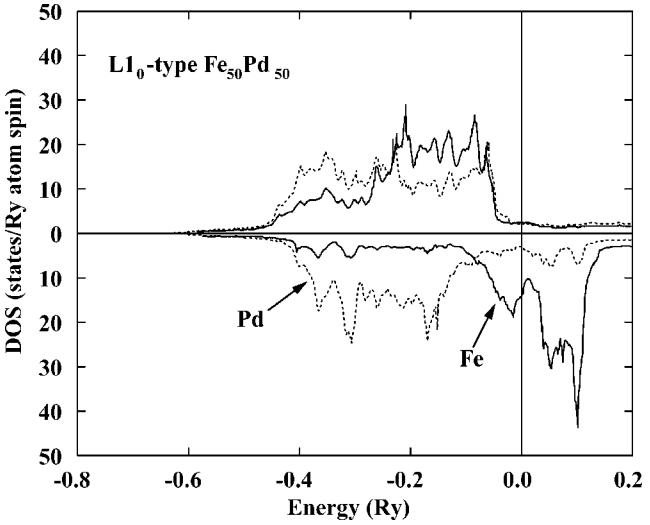

FIG. 8. The density of states calculated by the LMTO-ASA method for $L1_0$-type $Fe_{50}Pd_{50}$. The solid and dotted lines stand for the results for Fe and Pd, respectively.

of ca^2 is fixed to be the experimental value for $L1_0$-type $Fe_{50}Pd_{50}$ in order to separate the effect of the axial ratio c/a on the MAE from that of the volume. The calculated values of MAE for $x=50$ are in accord with the experimental results. In the region of $c/a>0.8$, the value of MAE becomes smaller as the ratio of c/a is apart from unity, or as $\sqrt{2}c/a$ is close to unity. The axial ratio dependence of MAE in the calculations qualitatively corresponds to the experimental results shown in Fig. 6. The MAE as a function of the band filling q in $L1_0$-type FePd is drawn in Fig. 10. The actual electron number in the unit cell of the $L1_0$-type FePd is 18, giving the local maximum in the MAE curve. Accordingly, the MAE decreases with increasing the value of q. This behavior would result from the decrease in anisotropy in the orbital angular momentum ΔL for $L1_0$-type $Fe_{50}Pd_{50}$.[31]

With increasing Pd concentration, the d electron number as well as the axial ratio c/a goes away from those in the equiatomic state. The decrease of the axial ratio has a similar effect on the MAE to the increase of the band filling and the

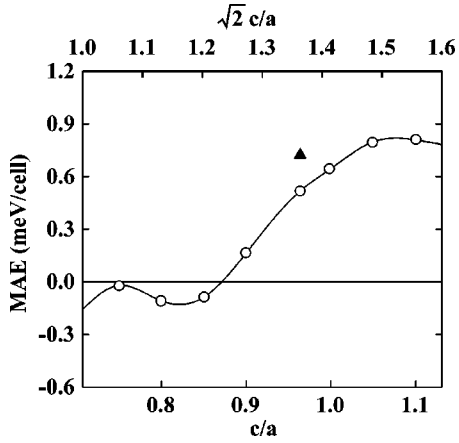

FIG. 9. The calculated MAE as a function of the axial ratio c/a for $L1_0$-type $Fe_{50}Pd_{50}$. The experimental result of MAE is represented by the symbol ▲.

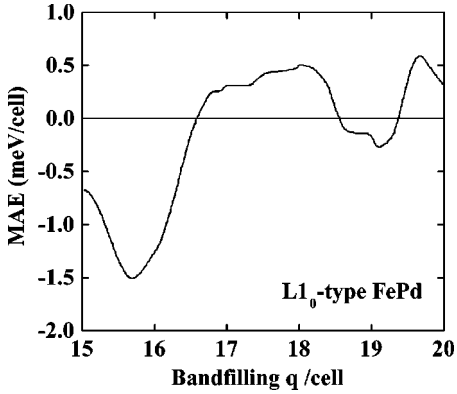

FIG. 10. The calculated MAE as a function of the band filling q for $L1_0$-type $Fe_{50}Pd_{50}$ alloy.

shift of the Fermi energy.[32] On the basis of a rigid band model, the value of band filling increases with the Pd concentration, resulting in the decrease in the MAE. For the calculation of the K_U curves in Fig. 9, the d electron number is fixed, and hence the MAE decreases with the ratio of c/a. According to the calculated results of K_U shown in Fig. 10, the MAE decreases with increasing the d electron number under the condition of the fixed axial ratio of c/a. Therefore, the present experimental results of the MAE which decrease with increasing Pd concentraion can be regarded as a corporative phenomenon between the increase in the tetragonal lattice distortion and the d electron number. All the above calculations of the MAE were based on the fourth theorem instead of the total energy calculations. In the previous studies on the first principles calculations of MAE for the $L1_0$-type FePt, CoPt, and FePd alloys, the discrepancy between the experimental and calculated values by the fourth theorem[31,32] is less than that with the total energy calculation.[30] In concrete, the calculated value of MAE using the total energy calculation with the LSDA is about 5 times larger than the experimental result,[30] whereas the calculated value of MAE using the fourth theorem with the LSDA is only 2 times larger than the experimental results.[31,32] Furthermore, in the total energy calculations with the generalized gradient approximation for $L1_0$-type $Fe_{50}Pd_{50}$, the direction of easy axis becomes perpendicular to the c axis,[30] different from the experimental result. Considering these results, the present calculations on the MAE stated above are reliable, even though the fourth theorem was used.

IV. CONCLUSION

The relation between the axial ratio and the magnetocrystalline anisotropy has been investigated both experimentally and theoretically. The $L1_0$-type FePd single crystals with a high degree of the long-range order in a single variant state were prepared by a heat treatment under compressive stress. The lattice constant of the a axis increases with the Pd concentration x, whereas that of the c axis is hardly changed. As a result, the axial ratio c/a increases with the Pd concentration x. The uniaxial magnetocrystalline anisotropy constant K_U was directly calculated from the difference between the

Helmholtz free energy along the a and c axes, which decreases with increasing x. Regarding the axial ratio as $\sqrt{2}\ c/a$ in the B2 representation the value of K_U decreases as $\sqrt{2}\ c/a$ becomes close to unity, that is, the nondistorted cubic B2 structure. The value of K_U at 4.2 K for the equiatomic composition is evaluated to be 2.1×10^7 erg/cm^3.

The electronic structure for the $L1_0$-type $Fe_{50}Pd_{50}$ has been evaluated from the first principles calculations with the LMTO-ASA method. The enhancement of the spin magnetic moment of the Fe atom is originated from the strong hybridization between the minority spin d bands of Fe and Pd. The calculated magnetocrystalline anisotropy energy MAE as a function of the axial ratio c/a qualitatively corresponds to the experimental results of the uniaxial magnetocrystalline anisotropy constant K_U. The increase in the d electron number due to increasing Pd concentration is regarded as the decrease in the ratio of c/a, resulting in the decrease in K_U.

ACKNOWLEDGMENT

The authors wish to thank Professor O. Kitakami of Institute of Multidisciplinary Research for Advanced Materials, Tohoku University for valuable discussions.

*Corresponding author. Electronic address: hisashi@maglab.material.tohoku.ac.jp

[1] R. Hultgren and C. A. Azpffe, Z. Kristallogr. **99**, 509 (1938).
[2] D. Ravelosona, A. Cebollada, F. Briones, C. Diaz-Paniagua, M. A. Hidalgo, and F. Batallan, Phys. Rev. B **59**, 4322 (1999).
[3] O. Klein, Y. Samson, A. Marty, S. Guillous, M. Viret, C. Fermon, and H. Alloul, J. Appl. Phys. **89**, 6781 (2001).
[4] P. R. Aitchison, J. N. Chapman, V. Gehanno, I. S. Weir, M. R. Scheinfein, S. McVitie, and A. Marty, J. Magn. Magn. Mater. **223**, 138 (2001).
[5] K. Sato and Y. Hirotsu, J. Appl. Phys. **91**, 8516 (2002).
[6] K. Sato and Y. Hirotsu, J. Appl. Phys. **93**, 6291 (2003).
[7] K. Chesnel, M. Belakhovsky, F. Livet, S. P. Collins, G. van der Laan, S. S. Dhesi, J. P. Attane, and A. Marty, Phys. Rev. B **66**, 172404 (2002).
[8] A. Kussmann and K. Müller, Z. Angew. Phys. **17**, 509 (1964).
[9] N. Miyata, H. Asami, T. Mizushima, and K. Sato, J. Phys. Soc. Jpn. **59**, 1817 (1990).
[10] A. Y. Yermakov and V. V. Maykov, Fiz. Met. Metalloved. **5**, 201 (1990); Phys. Met. Metallogr. **69**, 198 (1990).
[11] B. Zhang, T. Klemmer, D. Hoydick, and W. A. Soffa, IEEE Trans. Magn. **30**, 589 (1994).
[12] L. M. Magat, A. S. Yermolenko, G. V. Ivanova, G. M. Makarova, and Y. S. Shur, Fiz. Met. Metalloved. **26**, 511 (1968).
[13] B. Zhang and W. A. Soffa, Scr. Metall. Mater. **30**, 683 (1994).
[14] T. Ichitsubo, N. Nakamoto, K. Tanaka, and M. Koiwa, Mater. Trans., JIM **39**, 24 (1998).
[15] K. Tanaka, T. Ichitsubo, M. Amano, M. Koiwa, and K. Watanabe, Mater. Trans., JIM **41**, 917 (2000).
[16] A. Sakuma, J. Phys. Soc. Jpn. **63**, 1422 (1994).
[17] M. Weinert, R. E. Watson, and J. W. Davenport, Phys. Rev. B **32**, 2115 (1985).
[18] X. Wang, D. Wang, R. Wu, and A. J. Freeman, J. Magn. Magn. Mater. **159**, 337 (1996).
[19] T. Takezawa and T. Yokoyama, J. Jpn. Inst. Met. **45**, 1112 (1981).
[20] A. Kusmann and K. Jessen, Z. Metallkd. **54**, 504 (1963).
[21] R. Hultgren and C. A. Zaffe, Trans. AIME **133**, 58 (1939).
[22] K. Tanaka, T. Ichitsubo, and M. Koiwa, Mater. Sci. Eng., A **312**, 118 (2001).
[23] F. C. Nix and W. Shockley, Rev. Mod. Phys. **10**, 1 (1938).
[24] V. V. Maykov, A. Y. Yermakov, G. V. Ivanov, V. I. Khrabrov, and L. M. Magat, Fiz. Met. Metalloved. **67**, 79 (1989); Phys. Met. Metallogr. **67**, 76 (1989).
[25] B. W. Roberts, Acta Metall. **2**, 597 (1954).
[26] A. Y. Volkov, B. A. Greenberg, L. A. Rodionova, G. M. Gushcin, I. N. Sakhanskaya, N. I. Vlasova, and Y. I. Filippov, Phys. Met. Metallogr. **95**, 355 (2003).
[27] T. Klemmer, D. Hoydick, H. Okumura, B. Zhang, and W. A. Soffa, Scr. Metall. Mater. **33**, 1793 (1995).
[28] H. Shima, K. Oikawa, A. Fujita, K. Fukamichi, and K. Ishida, J. Magn. Magn. Mater. **272–276**, 2173 (2004).
[29] H. B. Callen and E. Callen, J. Phys. Chem. Solids **27**, 1271 (1966).
[30] I. Galanakis, S. Ostanin, M. Alouani, H. Dreyssé, and J. M. Wills, Phys. Rev. B **61**, 599 (2000).
[31] G. H. O. Daalderop, P. J. Kelly, and M. F. H. Schuurmans, Phys. Rev. B **44**, 12 054 (1991).
[32] A. Sakuma, J. Phys. Soc. Jpn. **63**, 3053 (1994).